Introduction to the Theory of Confinement

X. Garbet

Assoc. Euratom-CEA, CEA/DSM/DRFC CEA-Cadarache

Abstract. This introduction presents the main instabilities responsible for turbulence in tokamak plasmas, and the prominent features of the resulting transport. The usual techniques to construct reduced transport models are described. These models can be tested by analysing steady state and transient regimes. Another way to test the theory is to use a similarity principle, similar to the one used in fluid mechanics. Finally the physics involved in the formation and sustainment of transport barriers is presented.

Keywords: Turbulence, transport, tokamaks

1. INTRODUCTION

Understanding turbulent transport in magnetised plasmas is a subject of utmost importance to analyse and optimise experiments in present fusion devices, and also to design a future reactor. This appears as a fact when looking at the condition for getting a fusion power that is larger than the losses, the Lawson criterion, which states that the triple product $nT\tau_E$ must be larger than $6.10^{21}\mathrm{m}^{-3}\mathrm{keVs}^{-1}$ (n is the density, T the temperature, τ_E is the confinement time defined as the ratio of the energy content to power losses). It turns out that the confinement time τ_E, which is basically a thermal relaxation time, is mainly determined by conductive losses, and therefore by turbulent transport. A vigorous and coordinated effort has been undertaken worldwide to improve our knowledge in this domain. This lecture is an introduction to this subject.

The main instabilities that underlie turbulent transport in fusion plasmas are now well identified. The basic equations describing magnetized plasma turbulence are presented here. The most advanced simulations are done in the gyrokinetic framework, and have done a tremendous progress in the recent years. It will be seen that turbulence simulations have allowed an assessment of dimensionless scaling laws. The main results will also be summarized concerning the various transport channels. However gyrokinetic simulations turn out to be very demanding in terms of computational resources for a realistic simulation for ITER. Hence it has appeared necessary to develop reduced transport models.

The methodology for addressing this problem relies on an assumption of space and time scale separation between equilibrium and fluctuations. This assumption is the justification for developing a mean field theory of transport. A common recipe for building most models of transport is based on a quasi-linear theory combined with a mixing-length rule. Transport models are usually tested by comparing the predicted profiles to experimental data. An alternative powerful technique consists in analyzing

CP1095, *2nd ITER International Summer School: Confinement*
edited by: S.-I. Itoh, S. Inagaki, M. Shindo, and M. Yagi

transients, in particular heat modulation experiments. It appears that the accuracy of most transport models do not exceed 20% in conventional plasmas, and is certainly much worst in transient plasmas. This fact suggests that a mean field theory might not be appropriate for describing turbulent transport in tokamaks. This boils down to issues such as intermittency, turbulence self-organization, structure dynamics and non diffusive transport, which will be briefly addressed in this survey.

An important issue for fusion plasmas is to reach situations where the turbulent transport is low, i.e. where confinement is improved. Transport barriers, which are regions where turbulence is reduced or quenched, are now routinely produced and maintained in tokamaks. Flow shear and/or magnetic shear play a central role in the formation and sustainment of these transport barriers. These regimes are usually reached above a critical value of the heating power, which should be minimized.

This paper is not intended to be an exhaustive overview of all these topics, but rather an introduction that should encourage the reader to explore the more extensive reviews quoted in the text. The remainder of this paper is organized as follows. Section II briefly presents some general features and properties of turbulence in core tokamak plasmas. Dimensionless analysis is addressed in section III. The questions of reduced transport models and turbulence self-organization are treated in sections IV and V, while the status of our understanding from simulations is given in section V. The physics of transport barriers is sketched in section VII. A conclusion follows.

2. A BRIEF SURVEY OF MICRO-STABILITY

2.1. Geometry and plasma equilibrium

It is reminded here that field lines in a tokamak are helical and are winded on torii, called magnetic surfaces. These magnetic surfaces are nested around a magnetic axis (see Fig.1). Each magnetic surface is labeled by an effective radius r, which is a function of the poloidal flux. The set of coordinates is completed by toroidal and poloidal angles φ and θ. The poloidal angle can be chosen such that the winding number q of the field lines, called safety factor, is constant on each magnetic surface, i.e. depends on r only (a mathematical definition of the winding number is $q(r)=\boldsymbol{B}\cdot\nabla\varphi/\boldsymbol{B}\cdot\nabla\theta$, where $\boldsymbol{B}$ is the equilibrium magnetic field). At the very edge of the plasma, field lines are intercepted by plasma facing components, i.e. are open. The magnetic surface separating the region where field lines are closed from the region where they are open is called separatrix. Also the modulus of the magnetic field decreases with the major radius. This is an important feature of the magnetic field topology. As a consequence, charged particles with low parallel velocities exhibit a bouncing trajectory in the minimum of the field. These particles are called trapped particles and play an important role in the instabilities that underlie turbulence. However trapped particles are sensitive to collisions, which lead to velocity scattering, and therefore may detrap them, thus weakening their contribution to instabilities.

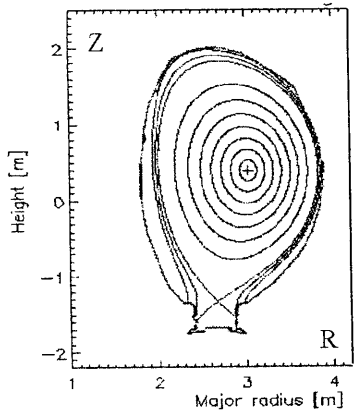

FIGURE 1. Set of nested magnetic surfaces in a poloidal plane of the JET tokamak. The configuration is axisymmetric around the vertical axis (toroidal direction).

The description of transport in tokamaks usually relies on time and spatial scale separation. Mean fields are the density, velocity and pressure (or temperature), averaged over fast time and spatial scales (in practice over poloidal and toroidal angles). These quantities, called equilibrium profiles, depend on the radius only and evolve on time scales much longer than a typical turbulence correlation time (~10μs). Hence this averaging procedure allows writing transport equations in the radial direction (1D mean field theory). Fig.2 shows schematic examples of pressure profiles for different operation regimes in a tokamak. Transport barriers develop in tokamak plasmas when appropriate conditions are met (usually when the heating power exceeds a critical value). A transport barrier will be defined here as a region where turbulence is strongly reduced, ideally quenched. Turbulence reduction leads to a decrease of transport coefficient, and therefore to profile steepening. This property can be easily verified from the Fourier law relating the heat flux to the temperature gradient: at constant flux, a decrease of the thermal conductivity leads to an increase of the temperature gradient. Two situations occur in tokamaks: edge transport barriers (originally called H-mode for "High" confinement) and internal transport barriers (ITBs) (see Fig.2 for typical shapes of profiles in this case).

2.2. Micro-instabilities

The spectrum of instabilities in tokamaks is quite complex. We will restrict the discussion here to core turbulence, except when discussing edge transport barriers. Core plasma micro-instabilities are in essence interchange-like modes. An interchange mode is unstable when the gradient of magnetic field is aligned with the gradient of equilibrium pressure. In this case the exchange of two flux tubes around a field line releases free energy. Such a situation occurs in a tokamak on the "low field side" (it is reminded here that the modulus of the magnetic field decreases with the major radius in a tokamak). Conversely the plasma is locally stable with respect to interchange on

the "high field side". Also trapped particles are localized on the low field side, as this corresponds to the place of minimum field along the field lines. Hence trapped particles are expected to play a prominent role in the interchange process. Last, but not the least, field lines connect locally stable and unstable regions. This process leads to modes which tend to be aligned along the equilibrium magnetic field. In other words, the typical transverse size (~10^{-2}m) of a mode is much smaller than its wavelength along the magnetic field (~10m). This feature persists in non linear regime. Hence turbulence in tokamak plasmas is quasi-2D. 3D effects cannot be ignored though, as the direction of the magnetic field changes spatially (magnetic shear). The detailed stability analysis is beyond the scope of this introduction. The most prominent features will be presented here.

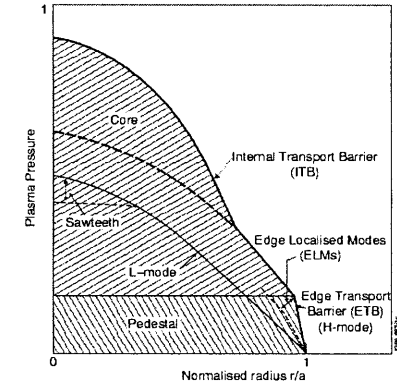

FIGURE 2. Schematic pressure profiles in a tokamak. Standard conditions correspond to "L-mode" plasmas. Transport barriers may develop in the edge ("H-mode"), and/or in the core (Internal Transport Barriers, ITBs).

For the sake of simplicity, we will restrict this survey to the main low wave number electrostatic micro-instabilities in core plasmas: Ion Temperature Gradient (ITG) driven modes and Trapped Electron Modes (TEM) [1,2] (called here ion and electron modes for simplicity). Electrostatic means that perturbations of the magnetic field are ignored, so that only the perturbed electric field matters. This assumption is appropriate if the plasma beta $\beta=2\mu_0 p/B^2$ (p is the total pressure, and B the magnetic field) is lower than the instability threshold for electromagnetic interchange modes (called "kinetic ballooning modes" [3] or Alfvén Ion Temperature Gradient modes [4,5]). The onset of ballooning modes is nevertheless believed to be potentially responsible for the degradation of confinement at high β. This state should indeed correspond to an Alfvénic (MHD) turbulence, and correspondingly a strong degraded confinement. Hence it is possible that the β limit in a tokamak might actually be linked in some cases to a strong MHD turbulence rather than MHD macroscopic instabilities. The electrostatic assumption is also questionable in the edge of tokamaks, where electromagnetic effects are known to be important [6,7]. The question of the β

dependence of edge turbulence is in fact a controversial subject. The high wave numbers instabilities [8,9,10], called Electron Temperature Gradient modes are also ignored for the moment. However it must be kept in mind that these modes may contribute significantly to electron transport for dominant electron heating. This question is discussed in section VI.

ITG/TEM modes are unstable in the limit of large wavelengths such that $k_\perp\rho_i<1$, where $k_\perp$ is the perpendicular wave number and ρ_i is the ion Larmor radius ($\rho_i=(m_iT_i)^{1/2}/e_iB$ where m_i is the ion mass, and T_i is the ion temperature, e_i the ion charge). In the non-linear regime, they produce particle, momentum, electron and ion heat transport. An important property of these micro-modes is the existence of an instability threshold. For a given profile of safety factor, the threshold of a pure ion mode (i.e. when the electron response follow a Boltzmann law) appears as a critical ion temperature logarithmic gradient $-R\nabla T_i/T_i$ (R is the major radius) that depends on the logarithmic density gradient $-R\nabla n_i/n_i$, and on the ratio of electron to ion temperature T_e/T_i. An ion mode usually rotates in the ion diamagnetic direction (the ion diamagnetic velocity is $\boldsymbol{V}^*_{pi}=\boldsymbol{B}\times\nabla p_i/n_ie_iB^2$, where p_i is the ion pressure, n_i the ion density). Trapped electron modes usually rotate in the electron diamagnetic direction and are mainly driven through a resonant interaction of the modes with trapped electrons at the precession frequency. The threshold is a critical value of $-R\nabla T_e/T_e$ that depends on $-R\nabla n_e/n_e$ and the fraction of trapped electrons f_t. A separate treatment of ion and electron modes is usually an oversimplification. Nevertheless, there exists experimental situations where one branch is dominant, for instance when one species is hotter than the other.

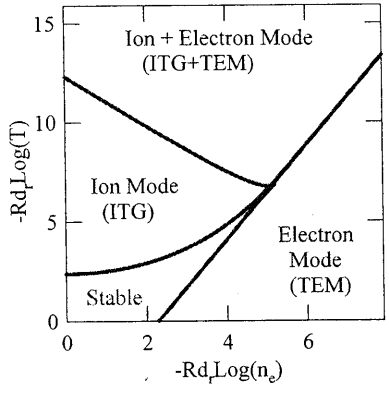

FIGURE 3. Stability diagram of ITG/TEM modes. Electron and ion temperatures and temperature gradient lengths are equal.

Fig.3 shows an example of stability diagram in the special case where the local electron and ion temperatures are equal, $T_e=T_i$, and their gradient lengths a well $L_{Te}=L_{Ti}$ (N.B. $L_T^{-1}=-\nabla T/T$) . Depending on the values of the gradient length, 0, 1 or 2

modes may be unstable. Well above all thresholds, both branches combine and the growth rate exhibits the typical expression for an interchange mode

$$\gamma_{lin}^2 = f_t\omega_{de}\omega^*_{pe} + \omega_{di}\omega^*_{pi} \qquad (1)$$

where $\omega^*_{ps}=k_\theta V^*_{ps}$ and $\omega_{ds}=2k_\theta\lambda_sV_{ds}$ (V_{ds} is the drift velocity due to the magnetic field curvature, $V_{ds}=-2T_s/e_sBR$, k_θ a poloidal wave number and $\boldsymbol{V}^*_{ps}=\boldsymbol{B}\times\nabla p_s/n_se_sB^2$ is called the diamagnetic velocity of the species 's'). The parameter λ_s depends on the magnetic shear $s=dLog(q)/dLog(r)$. More precisely, $\lambda_e=1/4+2s/3$ for trapped electrons and $\lambda_i=\langle cos(\theta)+s\theta sin(\theta)\rangle$ for ions, where the bracket indicates an average over the mode poloidal structure. There also exists a branch of ITG modes, which does not belong to the interchange family (slab ITG modes). The growth rate of slab ITG modes exhibits a scaling comparable to Eq.(1), but the amplitude is smaller.

2.3. Turbulence simulations

Turbulence has long been computed by using fluid equations [11]. For a strong and homogeneous magnetic field, the fluid equations are very close to those describing a 2D incompressible rotating fluid, where the electric potential plays the same role as the stream function, and the magnetic field replaces the rotation angular frequency. Starting from this idealized situation, several ingredients have been added progressively since the early 80's [12,13,14]: simulations are now 3D, describe several species including impurities, fluctuations are electromagnetic, and the full toroidal geometry is implemented. The status of 3D simulations can now be considered as satisfactory, although still progressing, in particular to avoid a separation between equilibrium and fluctuating quantities.

However, while plasmas are getting closer to the conditions for achieving fusion, they are less and less collisional since the collision frequency decreases with increasing temperature. In weakly collisional plasmas, charged particles experience resonant interactions with the electromagnetic field. These resonant processes cannot be described correctly by fluid equations. Hence the distribution function of each species must be computed by solving a kinetic (Vlasov) equation, coupled to Maxwell equations via charge and current densities. This means in principle solving a 6D problem (3 directions for space and 3 for velocities). In practice, the cyclotron motion of particles is much faster than the dynamics of turbulent structures. This allows averaging the equations over the fast cyclotron motion. A Vlasov equation can be written for the distribution function of gyrocenters. The new problem is now 4D (typically 3 coordinates for the gyrocenters, which is close to the centre of the cyclotron motion, and the parallel velocity), parameterized by a motion invariant (adiabatic invariant). This new Vlasov equation is called a gyrokinetic equation. Solving a 5D gyrokinetic equation for each species coupled to Maxwell equations is a very difficult problem due to the large range of scales that must be simulated. Nevertheless gyrokinetic simulations are now routinely run thanks to the progress made in the domains of supercomputers and numerical techniques (see refs. and [15] for overviews on the derivation of gyrokinetic equations and [16,17] for the state of

ıe art of numerical simulations). It turns out that gyrokinetic simulations are quite emanding in terms of computer resources. Hence less demanding techniques have een developed to predict the performances of devices. Two complementary pproaches are presented here, namely dimensionless scaling laws and reduced ·ansport models, before coming back to the results of simulations.

3. DIMENSIONLESS ANALYSIS

An important feature of turbulent transport is the existence of a similarity ·rinciple, which states that 3 dimensionless parameters, among many others, play a entral role, for given geometry and profile shapes [18,19] (an overview can be found n [20]). These principal dimensionless parameters are the normalized gyroradius $\rho_*=\rho_i/a$ (a is the minor radius), collisionality $\nu^*=\nu_{ei}qR/\varepsilon_a^{3/2}v_{Te}$ (ν_{ei} the electron-ion ollision frequency, $\varepsilon_a=a/R$ the inverse aspect ratio, v_{Te} is the thermal electron elocity) and plasma beta β. We note that for dimensional analysis the choice of lectrons or ions does not make any difference for the definition of ρ_*, since the mass atio is given (up to the mass number A, which leads to "isotope" effect, but whose lependence will not be considered here). However we will also define a normalized yroradius ρ_{s*} for each species 's', for quantitative purposes.

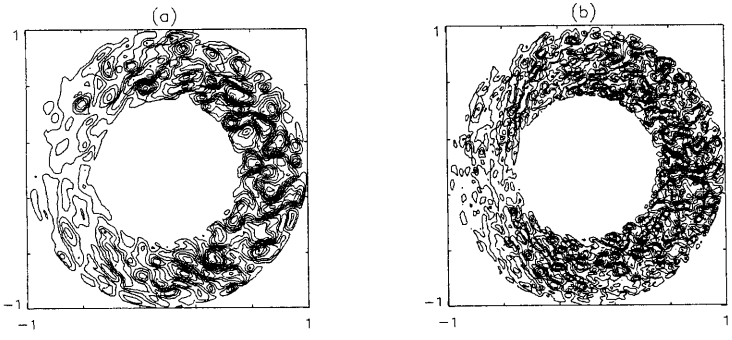

FIGURE 4. Contour lines of the electric potential calculated with 3D full torus simulations of ion urbulence for two values of the normalised gyroradius $\rho_*=1/50$ (a) and $\rho_*=1/100$ (b) [22]. The size of he vortices is proportional to ρ_*. This behaviour is consistent with a gyroBohm scaling law.

Let us consider ITG turbulence first. Simulations indicate that the scaling law s "gyroBohm" for small enough values of ρ_*. This means that correlation lengths, correlation times scale respectively as ρ_i, and R/v_{Ti}. Let us assume now that particle experience a random walk. In that case, the diffusion coefficient, which behaves as the square of a correlation length divided by a correlation time, should scale as $\rho_* T_i/eB$ (v_{Ti} is ion thermal speed $(T_i/m_i)^{1/2}$). This reference diffusion scaling is called gyroBohm diffusion and can also be written as

$$\chi_{i,gB} \equiv \frac{T_i}{eB}\frac{\rho_i}{a} \qquad (2)$$

Since early 3D fluid simulations of ion turbulence [21,22], and more recent gyrokinetic simulations [23,24,25], it is now widely admitted that the correlation length and time, and the heat flux follow the gyroBohm prediction in the limit of small values of ρ_* (see Fig.4 for an example). A departure from gyroBohm scaling is observed for a value of ρ_* above a critical value of ρ_*. The transport is then Bohm-like, i.e. the diffusion coefficient scales as T/eB. There is no consensus on the value of this critical normalized gyroradius and on the reason why the gyroBohm scaling is broken above this critical value.

The situation is less clear for β and collisionality parameters, because of competing effects. Collisionality has a stabilizing effect on electron (TEM) modes due to electron collisional detrapping [26,27]. On the other hand, collisional friction damps zonal flows [28,29], which are fluctuations of poloidal velocity that reduce turbulent transport (see section V).

The dependence on β is mainly a signature of electromagnetic effects, and is also involved in the compression of magnetic surfaces (the Shafranov shift, which is stabilizing, see section VII). In collisionless plasmas, increasing β stabilizes ITG/TEM modes. Above a critical value of β, (kinetic) ballooning modes become unstable [3]. Turbulence simulations basically confirm this behavior, i.e. a mild decrease of transport with increasing β, followed by a sharp increase of the diffusion coefficient above a critical value of β, of the order of half the ideal MHD β limit [30]. Hence it is expected that confinement should slightly improve when increasing β, then strongly degrades above some critical value of β. The value of this critical value does vary depending on plasma parameters [31]. Some recent gyrokinetic simulations indicate that in fact the ion heat transport is weakly sensitive to β, while the electron heat and particle diffusion coefficients are much more sensitive to electromagnetic effects [32]. This is an interesting finding, as it might explain why in usual cases where ion transport is dominant, no dependence is found experimentally. Nevertheless this question is in fact quite controversial and hotly debated both from the experimental and theoretical point of view.

Assuming a collisionless electrostatic turbulence, it appears that Eq.(2) can be transcribed into a very simple scaling law for the confinement time, i.e. $\omega_c\tau_E \equiv \rho_*^{-3}$ ($\omega_c=eB/m$ is the cyclotron frequency). This result can be compared to the ITER scaling (H-mode) $\omega_c\tau_E \equiv \rho_*^{-3.0}\beta^{-0.9}\nu_*^{0.0}$. It appears readily that the scaling for the normalized gyroradius fits, but that the experimental scaling law of the confinement time exhibits a strong β dependence, which suggests some role of electromagnetic instabilities. As mentioned before, this issue is debated.

4. TRANSPORT MODELS

Many transport models are built on the basis of linear stability considerations. They provide quantitative fluxes following two separate steps. The first one is based on a quasi-linear expression of fluxes. Considering for instance the particle flux $\Gamma_e=<n_e v_{Er}>$, where $\boldsymbol{v_E}=\boldsymbol{B}\times\nabla\phi/B^2$ is the $E\times B$ drift velocity (this is called "electrostatic" turbulence). The particle flux reads in Fourier space as

$$\Gamma_e = \sum_{k\omega} n_{e,k\omega} \frac{ik_\theta \phi^*_{k\omega}}{B} \qquad (3)$$

where $\phi_{k\omega}$ and $n_{k\omega}$ are Fourier components of perturbed electric potential and density.

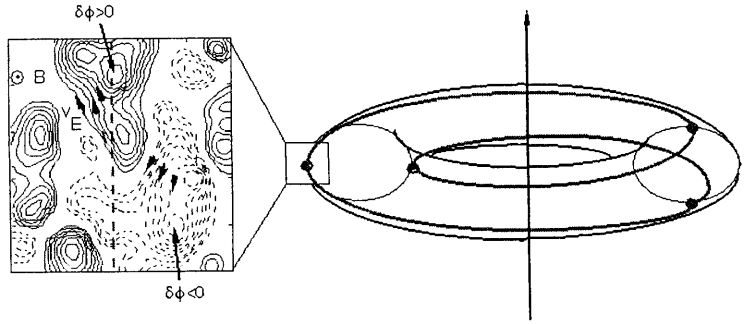

FIGURE 5. Random walk experienced by a charged particle in an electrostatic turbulence. The center of the cyclotron motion ("guiding center") approximately follows a field line (line in bold). The transverse velocity of the guiding center (mainly the electric drift velocity $v_E=B\times\nabla\phi/B^2$) fluctuates due to perturbations of the electric potential ϕ (contour lines of ϕ are shown in the box, a set of closed lines is called a "vortex", "eddy" or "convective cell"). This process leads to a diffusion and a transport coefficient of the order of $<|v_E|^2>\tau_c$, where τ_c is a typical correlation time.

The quasi-linear expression consists in replacing the Fourier component of the density by its linear expression calculated with linearized fluid or kinetic equations. Assuming a convection equation $\partial_t n_e+\nabla\cdot(n_e\boldsymbol{v_E})=0$ and a uniform magnetic field (implying incompressibility $\nabla\cdot\boldsymbol{v_E}=0$), the recipe given above yields a diffusive law $\Gamma_e=-D_{ql}dn_e/dr$. The quasi-linear diffusion coefficient D_{ql} is given by the expression

$$D_{ql} = \sum_{k\omega} \left| \frac{k_\theta \phi_{k\omega}}{B} \right|^2 \tau_{ck} \qquad (4)$$

where τ_{ck} is a correlation time as scale $1/k$, and the summation index runs over poloidal and toroidal wave numbers. This expression can be understood as a random walk estimate for a fluctuating velocity $v_{E,k\omega}=-ik_\theta\phi_{k\omega}/B$ (see Fig.5).

A similar exercise can be carried out for electron (respectively ion) heat flux $\phi_{Ee}=3/2<p_e v_{Er}>$ (respectively $\phi_{Ei}=3/2<p_i v_{Er}>$), leading to a thermal diffusivity $\chi_{e,i}=3/2D_{ql}$. In fact an advection equation is oversimplified, and the whole set of fluid or kinetic linearized equations must be kept when calculating the quasi-linear fluxes. It has to be noted that Eq.(3) depends on the level of potential fluctuations, which is unknown at this stage.

The second step consists of using a mixing-length rule to determine the level of fluctuations. The simplest version of this rule yields a level of fluctuation of the form $e\phi_k/T_e=1/k_\perp L_p$ (L_p is a pressure gradient length – here ϕ_k is an r.m.s. level averaged over time). This approximation is certainly the weakest part of the derivation of any transport model. For instance one would expect the level of fluctuation to vanish at the instability threshold. Various improvements have been proposed to account for these effects. A minimal improvement is to use an estimate that increases with the growth rate, i.e.

$$\frac{e\phi_{k\omega}}{T_e} = \frac{\gamma_k}{\omega^*_p} \frac{1}{k_\perp L_p} \qquad (5)$$

where γ_k is the linear growth rate at scale $1/k$ and ω^*_p the diamagnetic frequency. This expression combined with the above quasi-linear estimate and $\tau_{ck}\propto 1/\gamma_k$ yields the mixing-length diffusion coefficient

$$D_{ml} = \sum_k \frac{\gamma_k}{k_\perp^2} \qquad (6)$$

The Weiland [33] and GLF23 [34] models provide values of the linear growth rates γ_k. However they are based on fluid equations, which often predict values for the threshold that are too low. In fact the GLF23 model uses modified fluid equations to correct this drawback. Still the most accurate procedure to the calculate growth rates is to solve a kinetic equation to determine the plasma response [35,36]. The Weiland, GLF23, CDBM [37] and mixed Bohm-gyroBohm [38] models are the most widely used. Recently a quasi-linear model based on a simplified gyrokinetic calculation of growth rates has been developed [39].

An alternative picture emerges in the particular case where turbulent transport becomes very large when gradients cross the stability threshold. In this case, the profiles stay marginally stable, i.e. gradients are stuck to their critical value. This behavior is called "profile stiffness" [40]. In practice, only part of the profile is close to marginal stability. This concept is helpful to interpret experiments, when combined with linear stability analysis. An intermediate approach in between predictive transport modeling and strong profile stiffness consists of using a semi-empirical critical gradient model [41]. Assuming a gyroBohm scaling and electrostatic turbulence (see next section), a critical gradient model is of the form (for each species)

$$\chi_{cgm} = \chi_{gB}\left[\chi_s\left(\frac{-R\partial_r T}{T} - \kappa_c\right)H\left(\frac{-R\partial_r T}{T} - \kappa_c\right) + \chi_0\right] \qquad (7)$$

where $\chi_{gB}=q^{\nu}(T/eB)\rho_s/R$. Here χ_s is a number that characterizes the stiffness, κ_c, is the instability threshold, and $H(x)$ is a Heaviside function. Strong stiffness corresponds to a large value of χ_s. It is also assumed that a finite diffusivity persists when the gradient is below the threshold, with an amplitude χ_0. The safety factor q accounts for the improvement of confinement with plasma current. The value $\nu=3/2$ is presently the best compromise between various experiments. Hence a critical gradient model is characterized by 3 parameters only and is often used as a first analysis tool. Indeed the identification of these parameters is made possible by analyzing experiments where the heating source is modulated. Profile modulations give access to the heat pulse diffusivity $\chi_{hp}=\chi+\nabla T\partial\chi/\partial\nabla T$, and thereby provide a stringent test of transport models. It appears that the accuracy of transport models does not exceed 20% [42], which means that they should be improved. However, one faces very fundamental difficulties related to the complex behavior of turbulent transport. To quote only one difficulty, it is not even sure that transport is diffusive. These difficulties are briefly described in the following section.

5. TURBULENCE SELF-ORGANIZATION

Plasma turbulence self-organizes through the formation of (large scale) structures, which back-react on (small scale) fluctuations. Two types of structures play a crucial role: zonal flows, which are fluctuations of the poloidal velocity, and large scale transport events. These are rare but efficient events in terms of turbulent transport, as they trigger relaxations of the mean profiles. Structure dynamics leads to turbulence intermittency, which makes difficult the use of statistical theories, often based on an assumption of Gaussian (or near Gaussian) statistics. Hence intermittency can be considered as one reason why the predictive capability of the transport models based on a mixing-length assumption is limited.

5.1. Zonal flows

Zonal flows play an important role in turbulence simulations (for an overview see [43]). It was found that computations with radial modes ($k_\theta=0$, $k_\varphi=0$) of the electric potential are characterized by a transport lower than in simulations where these modes are artificially suppressed [44,45]. The mechanism which is often advocated for the generation of zonal flows is the Reynolds stress $\langle v_E v_E \rangle$, whose non zero divergence drives the plasma velocity in poloidal and toroidal directions. Another source of poloidal flow comes from flow compressibility (related to magnetic field curvature) [46]. These modes, called Geodesic Acoustic Modes (GAMs), have a frequency of the order of c_s/R, where c_s is the sound frequency. Hence the name Zonal Flows is now usually reserved to low frequency fluctuations of the poloidal flows, while GAMs are related to quasi-coherent modes at higher acoustic frequencies.

Another mechanism has been proposed [47,48] which relies on the Kelvin-Helmholtz instability. The point is that a vortex elongated in the radial direction (streamer) can drive a secondary instability of the Kelvin-Helmholtz type. This new structure corresponds to a sheared poloidal flow, which deletes the primary vortex. This mechanism has been much debated, as KH modes tend to be stabilized by the magnetic shear and are not expected to play an important role in normal conditions. Turning back to the generation via the Reynolds stress, it appears that in usual circumstances, the stress is proportional to the turbulence intensity times the zonal flow velocity. The proportionality coefficient is positive so that a flow amplification process takes place. Since the damping of poloidal flows is very small [49] (it is likely controlled by collisions), the amplitude of these flows tends to be large. Zonal flows back reacts on fluctuations via a shearing process: vortices are stretched by sheared flows, leading to a strong dissipation by the background diffusion. This process takes place provided that the zonal flow evolution time is longer than a vortex life time. Regarding this criterion, GAMs are expected to be less efficient than zonal flows. This stabilization process is similar to the vortex shearing stabilization due to a mean shear flow [50] (see also section VII). The turbulent generation of zonal flows, which back reacts on turbulence via shearing, is a very important process, which rules turbulence self-regulation.

5.2. Large scale transport events – Turbulence spreading

Several turbulence simulations exhibit large scale transport events, which enhance the anomalous transport. Two mechanisms have been identified: avalanches and streamers. Avalanches appear via a domino effect: if a gradient of temperature (or density) locally exceeds an instability threshold, it generates a burst of transport that expels some heat or matter, thus increasing the gradient on a neighboring radial position, where the same process may occur again. In this scheme, an excess of heat propagates downward, whereas a hole moves upward the mean gradient [51]. There is some similarity between this process and sand pile automatons proposed as a paradigm for Self-Organised Critical systems [51]. Avalanches are commonly observed in numerical simulations, in particular during transients [52,53,54,55]. The question of avalanches is closely connected to the concept of turbulence spreading [56,57]. One expects indeed that turbulence might spread from unstable to stable regions. The extent of the spreading region obviously depends on the growth rate and the turbulent diffusion coefficient, a tentative estimate being $\sqrt{D/\gamma_{lin}}$. During a transient, fronts are expected to mediate the spreading. The balance between growth and diffusion yields an estimate of the spreading velocity, $c_{front} \approx \sqrt{\gamma_{lin} D}$ [58,59]. Using Eqs.(1) and (2), it is found that c_{front} scales as $\rho_* c_s$, i.e. is a fraction of the sound speed. Fronts are a possible form of avalanches, and can be seen as the time dependent manifestation of turbulence spreading.

Streamers are convective cells that are elongated in the radial direction. They have also been observed in various turbulence simulations [60,10,61]. They are obviously competing with shear flows, since a streamer cannot survive to a strong

shear flow. It will be seen in the next section that they might play an important role in boosting the flux associated to small scale turbulence.

The existence of meso-scale structures, i.e. whose size is intermediate between a correlation length and the plasma size, raises several issues, namely the question of the validity of the assumption of locality, which underlies the diffusion/convection form of fluxes. It is stressed however that the existence of ballistic fronts do not necessarily contradict this form [58,59]. Also the Fokker-Planck form of transport equations is very robust [62]. Nevertheless, this question is legitimate and several non-local models have been proposed in the literature [63,64,65], often based on fractional kinetic approach. The question of locality is quite debated and remains an open question.

6. MAIN RESULTS OBTAINED FROM TURBULENCE SIMULATIONS

6.1. Ion heat transport

Ion heat transport was addressed first by simulations and can be considered as a mature subject. In fact, the computation of the ion heat diffusivity has become with time a way of comparing code. This was done in the US within the frame of the CYCLONE project [66], and in Europe within the frame of the TF-ITM IMP4 project [67]. Several results came out of these exercises. First the actual threshold was found to be larger than the linear stability threshold (Dimits shift). This is due to the onset of a regime where zonal flows dominate and prevent the onset of turbulence. Second the heat diffusivity was found to match the following approximate relation

$$\chi_i = 7.9\chi_{i,gB}\left(1-6\frac{L_{Ti}}{R}\right) \qquad (8)$$

where L_{Ti} is the temperature gradient length. Finally it was found in the CYCLONE case that gyrokinetic simulations found heat diffusivities lower that the kinetic values. This is one of the main reasons why most of the effort was focused on gyrokinetic calculations afterwards. In the TF-ITM project, some one of the fluid simulations was below the CYCLONE fit Eq. (8). Nevertheless the same trend remains qualitatively true.

6.2. Electron heat transport

Electron heat transport is less consensual than heat transport. First it is stressed that pure ITG transport leads to some amount or electron transport. Nevertheless it is found that the corresponding contribution is too small to explain the heat diffusivity observed when electron heating is dominant (e.g. Electron Cyclotron Resonant Heating). Hence it is expected that trapped electron modes (TEM) and/or electron temperature gradient (ETG) driven modes play some role.

Gyrokinetic simulations show indeed that TEM modes contribute to electron transport above the stability threshold [68]. The diffusivity can be fit by a formula of

the type Eq.(3). Some comparison with experiments has been done. A prominent feature of TEM turbulence is its sensitivity to collisionality. Electrons trapped in minima of the magnetic field get untrapped by collisions. This leads to a decrease of the heat diffusivity.

The question of ETG driven turbulence is much more controversial. If one assume an homothetic behavior to ITG turbulence, the gyroBohm estimate Eq.(2) predicts an electron diffusion coefficient that is $(m_e/m_i)^{1/2}$ smaller that the ion heat diffusivity. Since the measured electron diffusion coefficient is of the same order as the ion value, it appears that the expected value for ETG turbulence is too small by an order of magnitude. However it is was argued in [10] that zonal flows has little influence on small structures, hence favoring the emergence of streamers, which can enhance by much this value since they correspond to large scale transport events. The question of streamers has then been subject to a hot debate. Although it looks like that there is an agreement on their existence, the enhancement factor associated to streamers vary a lot in the literature [69,70,71,72]. It was recently mentioned that the question of pure ETG turbulence is an ill-posed problem [73,74]. Simulations of the whole spectrum of instabilities (ITG, TEM, ETG) with the GYRO code showed that in fact the contribution to ETG modes to the electron diffusivities is less than 10% in a typical case [75]. This was confirmed by a recent simulation with the GENE code where a similar number was found when electron and ion temperature gradient lengths are the same [76]. However it is also found on the latter work that when the electron temperature gradient length is larger, ETG modes can contribute significantly to electron turbulent transport.

6.3. Particle transport

Particle transport is obviously an important question for next step devices. On the one hand, one would like the density to be the highest as possible to enhance the fusion power. Since the edge density must remain low enough to avoid a disruption (Greenwald limit), one would like to produce peaked density profiles. On the other hand, peaked density profiles might lead to impurity neoclassical accumulation. One key characteristic of the particle flux is that it cannot be correctly described by a pure diffusion. Indeed it is well known that density profiles are peaked, even when the ionization source is localized in the edge. To explain this behavior, the particle flux is traditionally written as $\Gamma = -D\nabla n + Vn$ [77], where V is the pinch velocity and D is the particle diffusion coefficient. Fluid and gyrokinetic simulations (quasi-linear and fully non linear) show indeed that a finite pinch velocity is driven by turbulence. This velocity contains a "curvature" (or "compressional") term, and thermodiffusion contribution, i.e. schematically [78]

$$\frac{VR}{D} = C_{curv} + C_{\nabla T}\frac{R\nabla T}{T} \qquad (9)$$

The coefficient C_{curv} is related to compressional effects and is well described by turbulence equipartition theory [79,80]. It can be shown that when trapped electrons behave as trace particles in a dominant ITG turbulence, one has $C_{curv} = 2\lambda_e = 1/2 + 4s/3$.

Hence the curvature pinch introduces a link between the density and safety factor profile. The thermodiffusion coefficient C_{VT} can be shown to change of sign with the phase velocity of fluctuations (up to an off-set), i.e. when moving for instance from ITG to TEM dominant turbulence (see Fig.6). Typically, the thermal pinch velocity is directed outward ($C_{VT}<0$) for ITG turbulence. It is stressed that particle transport simulation requires simulating both electrons and ions (obviously the particle flux $\langle nv_E \rangle$ cancels is one of the species is adiabatic). Collisionality plays an important role in that matter. Indeed the ratio *VR/D*, which is representative of the peaking factor of the density, decreases as 1/ν* [81].

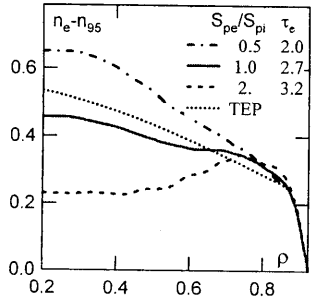

FIGURE 6. Density profiles when varying the ratio of electron to ion heating S_{pe}/S_{pi}=*0.5, 1* and *2*. The corresponding values of τ_e at ρ=*0.5* are indicated.

A related question is the issue of impurity transport. In that case again, a pinch velocity is driven by turbulence. Here it is found that the thermodiffusion coefficient is directed outward for ITG turbulence, which is favorable. Unfortunately the coefficient of the thermodiffusion term decreases as *1/Z*, where *Z* is the charge number [82]. Hence it is negligible for heavy impurities. The compressional term contains a term due to perpendicular and parallel compressibility [83]. The pinch velocity due to perpendicular compressibility is constant and directed inward, while the associated to parallel compressibility scales as *Z/A*, and its sign depends on the phase velocity of the fluctuations. It is outward for dominant TEM turbulence. Gyrokinetic simulations are roughly in agreement with the global picture [84], although a more quantitative assessment of the dependence on charge and mass numbers is needed.

As a final note, the reader should keep in mind that neoclassical theory predicts a pinch velocity for electrons (Ware pinch) and impurities (typically proportional to the main ion density gradient, up to a thermal screening term). However in many cases, these terms are subdominant, except in transport barriers, or close to the magnetic axis where turbulence is weak since the gradients are usually below the critical stability thresholds.

6.4. Momentum transport

Momentum transport has been investigated only quite recently. These studies were motivated by the discovery of plasma "spontaneous" spin-up, i.e. situations

where a significant toroidal rotation was measured, in absence of any external torque. Moreover, in many case co-rotation was observed (toroidal velocity in the same direction as the current), which cannot be explained by simple effects as ripple losses or direct losses of ions in the edge. Theory predict of flux of parallel momentum of the form $\Gamma_U / n_i = -\chi_u \nabla U_{//} + V_U U_{//} + S_U$. The parallel velocity $U_{//}$ is not identical to the toroidal velocity, but close enough to get an idea of the various processes at work. When compared to the expression for particle transport, an extra term S_U appears, called residual stress. The pinch velocity V_U is associated to curvature and to thermodiffusion [85,86]. It was also proposed that the Coriolis force contributes to this pinch [87]. Gyrokinetic simulations show that a pinch velocity and residual stress exist. However the values found for these contributions are relatively modest [88]. Work is actively been done to understand the various mechanisms at play.

7. TURBULENCE CONTROL AND TRANSPORT BARRIERS

The physics of transport barriers is a broad subject that is already covered by several overview papers for external [89,90,91,92] and internal transport barriers [93,94,95]. Two generic key parameters are known to play a central stabilizing role: flow shear and magnetic shear. Other ingredients may be involved (density gradient, ratio of electron to ion temperature, impurity content, ...), but are less generic than flow and magnetic shears.

7.1. Shear flow stabilization.

The physics of turbulent transport reduction due to $E \times B$ shear flow is well documented. The interested reader may consult overviews on theory [50] and experiments related to shear flow stabilization [96]. Stabilization results essentially from the shearing of turbulent convective cells. An approximate criterion for stabilization is $\gamma_E > \gamma_{lin}$ [97], where γ_E is the flow shear rate defined as (in a simplified geometry)

$$\gamma_E = \frac{d}{dr}\left(\frac{E_r}{B}\right) \tag{10}$$

and γ_{lin} is the maximum linear growth rate. Here B is the magnetic field and E_r is the radial electric field. A second criterion [98] consists in comparing a phase decorrelation time (Dupree time) to a turbulence correlation time

$$\left[k_\theta^2 \gamma_E^2 D\right]^{1/3} \tau_c > 1 \tag{11}$$

where D is a diffusion coefficient and τ_c a turbulence auto-correlation time. The latter criterion requires measurements of D and τ_c, and is therefore more difficult to assess. Both criterions (10) and (11) are equivalent when using a mixing-length estimate for the diffusion coefficient and assuming $\gamma_{lin}\tau_c = 1$. The radial electric field is constrained by the ion force balance equation

$$E_r = \frac{T_i}{e_i}\frac{dn_i}{n_i dr} + (1 - k_{neo})\frac{dT_i}{e_i dr} + V_\varphi B_\theta \qquad (12)$$

where the number k_{neo} depends on the collisionality regime and V_φ is the ion toroidal velocity. Once a barrier is formed, a positive loop takes place where density and ion temperature gradients increase, thus boosting the velocity shear rate.

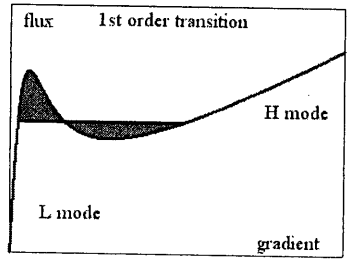

FIGURE 7. 1st order transition describing the L-H transition.

A simple model can be written to describe a barrier formation due to shear flow. To account for the stabilising effect of a shear flow, we use a diffusion coefficient of the form (see [99,100])

$$D = \frac{D_0}{1 + \left(V_E' \tau_c\right)^2} \qquad (13)$$

where D_0 is a the turbulent viscosity without flow shear. Using Eq.(12) with $k_{neo}=1$ and no toroidal velocity, one gets a particle flux of the form

$$\Gamma = -\frac{D_0}{1 + C\left(\frac{dn}{dr}\right)^2}\frac{dn}{dr} - D_{coll}\frac{dn}{dr} \qquad (14)$$

where D_{coll} is the collisional viscosity. The parameter C depends in principle on many parameters, but we take it constant to simplify the analysis. Note also that D_{coll} is in principle very small, but it can be replaced by a background turbulence diffusion coefficient, for instance a small scale turbulence that is weakly sensitive to shear flow stabilisation. Drawing the particle flux versus the gradient of velocity exhibits an S-curve (see Fig,7). A bifurcation is therefore expected above a critical flux. It is sometimes called 1st order transition, by reference to the terminology of phase transitions. The criterion for the transition onset is still debated. A jump of gradient is expected at the critical flux that satisfies the Maxwell construction of equal area [101,102] (in the latter case, the S-curve appears for the radial electric field versus the gradients). A similar analysis can be done for other channels, although a complication comes from the coupling between the various channels. Also the bifurcation might

come from the dynamics of the radial electric field itself. It has been shown that this dynamics can be described by an S-curve as well [103].

One potential difficulty for next step devices is that the torque will be small, so that $V_\varphi \approx 0$. Since typical growth rates are of the order of c_s/a, it is found that the ratio γ_E/γ_{lin} scales as the normalized gyroradius ρ_*. This ratio is small in present tokamaks and will be even smaller in the next generation. This smallness is compensated in the edge by small values of the gradients length, which lead to a shear flow sufficient to trigger an external transport barrier above a critical value of the heat flux. The mechanisms at play are not entirely known to date. The situation is more complex for internal transport barriers. In this case, shear flow is usually not large enough by itself to trigger a barrier, and another mechanism is needed to lower the linear growth rate. Optimizing the magnetic configuration, for instance by modifying the magnetic shear, provides a mean to do that.

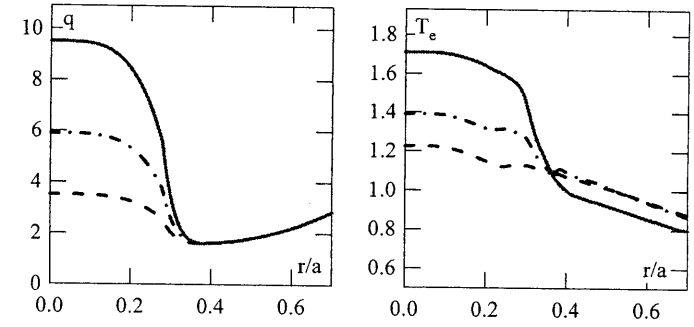

FIGURE 8. Profiles of safety factor, and electron temperature calculated with the TRB turbulence code [110].

7.2. Negative magnetic shear and α stabilization.

Negative magnetic shear is known to decrease the interchange drive [104]. This effect is enhanced by the Shafranov shift of magnetic surfaces (also called α effect, $\alpha = -q^2 R d\beta/dr$ is a measure of the Shafranov shift) [105,106]. In fact this physics is related to the stability of MHD modes [107,108] and the "access to second stability" (see for instance [109]). For electron modes, stabilization occurs when $s<-3/8$, consistently with Eq.(1), while for ions the exact value depends on the poloidal structure of modes. This stabilization scheme has been tested both with fluid and kinetic simulations. An electron transport barrier appears when the magnetic shear is negative, as shown on Fig.8 [110]. This effect is amplified for values of α of the order of unity. For electron modes, theory predicts stability when $s<3\alpha/5-3/8$. A similar effect exists for ions, which comes from the shear dependence of the ion curvature averaged over the mode structure $\lambda_i = \langle \cos(\theta) + (s\theta - \alpha \sin(\theta))\sin(\theta) \rangle$. However it is important to note that slab

ITG modes are not sensitive to these effects, and remain unstable at negative magnetic shear. The resulting turbulence is nevertheless weaker. It has to be noted that the nature of the transition changes as compared to shear flow triggered barriers. Indeed the stabilization via the magnetic configuration is essentially a linear process, that would lead in fact to a second order phase transition (no discontinuity in the gradient). Nevertheless, recent measurements indicate that the poloidal velocity is anomalous at the barrier onset, which suggest a prominent role of zonal flows. Hence, the picture given here is probably oversimplified.

8. CONCLUSION

Although many aspects of turbulent transport in fusion plasmas are now understood, several challenges still stand ahead. First, a fully predictive transport model does not exist yet although impressive progress has been made in this direction. It is likely that the mixing-length estimate, which is the main recipe that underlies most transport models, need to be modified in order to account for recent advances in the understanding of turbulence dynamics. Second, the ingredients leading to the formation and sustainment of transport barriers are not fully understood. It is clear that magnetic and flow shears are the main players that control transport barriers. However the conditions for their development remain unclear. This is particularly true for the flow shear in external transport barriers. Clearly some progress is needed, as transport barriers are mandatory to design reactors with a reasonable size. Finally turbulence dynamics still resists the impressive amount of studies and investigations done up to now. One difficulty is now identified as the complex behaviour of structures, which are responsible for intermittency. Turbulence simulations and fluctuation measurements have brought an invaluable input in this matter and progress is made every day. Still gyrokinetic, i.e. 5D, simulations are a formidable challenge in terms of computing resources, and also data analysis. Ultimately understanding the dynamics of turbulence should lead to a better control of transport. Control techniques based on the fine tuning of the magnetic configuration and flow shear in real-time are currently used in fusion devices. Whether more refined techniques can be used to control turbulence remains an open and challenging question.

REFERENCES

1. W. Horton, *Rev. Mod. Physics* **71**, 735 (1999).
2. J. Weiland, "*Collective Modes in Inhomogeneous Plasmas*", IOP, 2000.
3. G. Rewoldt, W.M. Tang, R.J. Hastie, *Phys. Fluids* **30**, 807 (1987).
4. F. Zonca, Liu Chen, J.Q. Dong, R.A. Santoro, *Phys. Plasmas* **8**, 1917 (1999).
5. G.L. Falchetto , J. Vaclavik and L. Villard, *Phys. Plasmas* **10**,1424 (2003).
6. S.J. Camargo , B.D. Scott, and D. Biskamp, *Phys. Plasmas* **3**, 3912 (1996).
7. B.N. Rogers, J.F. Drake, and A. Zeiler, *Phys. Rev. Lett.* **81**, 4396 (2000).
8. J.F. Drake, P.N. Guzdar, and A.B. Hassam, *Phys. Rev. Lett.* **61**, 2205 (1988).
9. W. Horton, B.G. Hong, W.M. Tang, *Phys. Fluids* **31**, 2971 (1988).
10. F. Jenko, W. Dorland, M. Kotschenreuther, B.N. Rogers, *Phys. Plasmas* 7, 1904 (2000). W. Dorland et al., Phys. Rev. Lett. **85**, 5579 (2000).
11. S.I. Braginskii, in *Reviews of Plasma Physics*, edited by M.A. Leontovitch (Consultants Bureau, New York, 1965), Vol.I, p.205.

12. W . Terry and W. Horton, *Phys. Fluids* **26**, 106 (1983).
13. R. E. Waltz, *Phys. Fluids* **26**,169 (1983).
14. A. Hasegawa and M. Wakatani, *Phys. Rev. Lett.* **50**, 683 (1983).
15. Y. Idomura, T.H. Watanabe and H. Sugama, *C. R. Physique* 7, 650 (2006).
16. L. Villard et al., *Plasma Phys. Control. Fusion* **46**, B51 (2004).
17. A.J. Brizard and T.S. Hahm, *Rev. Mod. Phys.* **79**, 421 (2007).
18. B.B. Kadomtsev, *Sov. J. Plasma Phys.* **1**, 295 (1975).
19. J.W. Connor, and J.B. Taylor, *Nucl. Fusion* **17**, 1047 (1977).
20. X. Garbet, AIP Conf. Proc. **1013**, 287 (2008).
21. X. Garbet, R.E. Waltz, *Phys. Plasmas* **3**, 1898 (1996).
22. M. Ottaviani and G. Manfredi, *Phys. Plasmas* **6**, 3267 (1999).
23. Z. Lin, S. Ethier, T. S. Hahm, and W. M. Tang, *Phys. Rev. Lett.* **88**, 195004 (2002).
24. J. Candy and R. E. Waltz, *Phys. Rev. Lett.* **91**, 045001 (2003).
25. V. Grandgirard, et al., *Plasma Phys. Control. Fusion* **49**, B173-B182 (2007).
26. B.B. Kadomtsev, O.P. Pogutse, *Reviews of Plasma Physics*, edited by M.A. Leontovitch (Consultant Bureau, New York, 1970) Vol. 5, p. 249.
27. F. Ryter et al., *Phys. Rev. Lett.* **95**, 085001 (2005).
28. P. H. Diamond et al., *Plasma Phys. Control. Fusion* **47**, R35 (2005).
29. Z. Lin, *Phys. Rev. Lett.* **88**, 195004 (2000).
30. P.B. Snyder, G.W. Hammett, *Phys. Plasmas* **8**, 744 (2001).
31. B. D. Scott, *New J. Phys.* **7**, 92 (2005).
32. J. Candy, *Phys. Plasmas* **12**, 072307 (2005).
33. H. Nordman, J. Weiland, A. Jarmen, *Nucl. Fusion* **30**, 983 (1990).
34. R.E. Waltz, G.M. Staebler, W. Dorland, et al., *Phys. Plasmas* **4**, 2482 (1997).
35. M. Kotschenreuther, W. Dorland, M.A. Beer, et al., *Phys. Plasmas* **2**,2381 (1995).
36. C. Bourdelle et al., *Nucl. Fusion* **42**, 892 (2002).
37. K. Itoh, S.I. Itoh, A. Fukuyama, *Phys. Rev. Lett.* **69**, 1050 (1992).
38. M. Erba et al., *Plasma Phys. Contr. Fusion* **39**, 261 (1997).
39. C. Bourdelle et al., *Phys. Plasmas* **14**, 112501(2007).
40. B. Coppi and N. Sharky, *Nucl. Fusion* **21**, 1363 (1981).
41. F. Imbeaux, F. Ryter and X. Garbet, *Plasma Phy. and Control. Fusion* **43**, 1503 (2001).
42. ITER Physics Expert Groups on Confinement and Transport and Confinement Modelling and Database, *Nucl. Fusion* **39**, 2175 (2000).
43. P.H. Diamond, S-I. Itoh, K. Itoh, and T.S. Hahm, *Plasma Phys. Control. Fusion* **47**, R35 (2005).
44. M.A. Beer, Ph. D. thesis, Princeton University 1995.
45. Z. Lin, et al., *Science* **281**, 1835 (1998).
46. K. Hallatschek and D. Biskamp, *Phys. Rev. Lett.* **86**, 1223 (20001).
47. B.N. Rogers, W. Dorland, and M. Kotschenreuther, *Phys. Rev. Lett.* **85**, 5336 (2000).
48. Y. Idomura, S. Tokuda, and M. Wakatani, *Phys. Plasmas* **7**,3551 (2000).
49. M. N. Rosenbluth and F.L. Hinton, *Phys. Rev. Lett.* **80**, 724 (1998).
50. P.W. Terry, *Rev. Mod. Phys.* **72**, 109 (2000).
51. P.H. Diamond and T.S. Hahm, *Phys. Plasmas* **2**, 3640 (1995).
52. B.A. Carreras, D. Newman, V.E. Lynch, and P.H. Diamond, *Phys. Plasmas* **3**, 2903 (1996).
53. Y. Sarazin, P. Ghendrih, *Phys. Plasmas* 5, 4214 (1998).
54. X. Garbet, Yet al., *Nucl. Fusion* **39**, 2063 (1999).
55. P. Beyer, S. Benkadda, X. Garbet, P.H. Diamond, *Phys. Rev. Lett.* **85**, 4892 (2000).
56. X. Garbet, L. Laurent, A. Samain, J. Chinardet, *Nucl. Fusion* **34**, 963 (1994).
57. T. S. Hahm, P.H. Diamond, Z. Lin, K. Itoh and S-I. Itoh, *Plasma Phys. Control. Fusion* **46**, A323 (2004).
58. O.D. Gürcan, P.H. Diamond, and T.S. Hahm, *Phys. Rev. Lett.* **97**, 024502 (2006).
59. X. Garbet, Phys. Plasmas **14**, 122305 (2007).
60. J.F. Drake, P.N. Guzdar, and A.B. Hassam, *Phys. Rev. Lett.* **61**, 2205 (1988).
61. P. Beyer, S. Benkadda, X. Garbet, P.H. Diamond, *Phys. Rev. Lett.* **85**, 4892 (2000).

62. D. F. Escande and F. Sattin, *Phys. Rev. Lett.* **99**, 185005 (2007).
63. D. del-Castillo-Negrete et al., *Phys. Rev. Lett.* **91**, 018302 (2003).
64. B. Ph. van Milligen, R. Sanchez, B. A. Carreras, *Phys. Plasmas* **11**, 2272 (2004).
65. T. Iwasaki et al. , *Nucl. Fusion* **39**, 2127 (1999).
66. A.M. Dimits et al., *Phys. Plasmas* **7**, 969 (2000).
67. G. Falchetto et al., to appear in *Plasma Phys. and Control. Fusion.*
68. T. Dannert and F. Jenko, *Phys. Plasmas* **12**, 072309 (2005).
69. Y. Idomura and M. Wakatani, *Phys. Plasmas* **7**, 3551 (2000).
70. B. Labit and M. Ottaviani, *Phys. Plasmas* **10**, 126 (2003).
71. J. Li and Y. Kishimoto, *Phys. Plasmas* **11**, 1493 (2004).
72. Z. Lin, L. Chen, F. Zonca, *Phys. Plasmas* **12**, 056125 (2005).
73. Y. Idomura, *Phys. Plasmas* **13**, 080701 (2006).
74. W. M. Nevins et al., *Phys. Plasmas* **13**, 122306 (2006).
75. J. Candy et al., *Plasma Phys. Controlled Fusion* **49**, 1209 (2007).
76. T. Görler and F. Jenko, *Phys. Rev. Lett.* **100**, 185002 (2008).
77. B. Coppi and C. Spight, *Phys. Rev. Lett.* **41**, 551 (1978).
78. X. Garbet, *Phys. Rev. Lett.* **91**, 035001 (2003).
79. V.V. Yankov, *JETP Lett.* **60**, 171 (1994).
80. M.B. Isichenko, A.V. Gruzinov, P.H. Diamond, *Phys. Rev. Lett.* **74**, 4436 (1996).
81. C. Angioni, A.G. Peeters, G.V. Pereverzev et al., *Phys. Plasmas* **10**, 3225 (2003) ;C. Angioni, A.G. Peeters, G.V. Pereverzev et al., *Phys Rev Lett.* **90**, 205003-1 (2003).
82. N. Dubuit et al., *Phys. Plasmas* **12**, 082511-1 (2005).
83. C. Angioni and A. G. Peeters, *Phys. Rev. Lett.* **96**, 095003(2006).
84. C. Estrada-Mila, J. Candy, and R. E. Waltz, *Phys. Plasmas* **12**, 022305 (2005).
85. O. D. Gürcan, P. H. Diamond, and T. S. Hahm, *Phys. Plasmas* **14**, 055902 (2007).
86. T. S. Hahm, P. H. Diamond, O. D. Gurcan, and G. Rewoldt, *Phys. Plasmas* **14**, 072302 (2007).
87. A. G. Peeters, C. Angioni, and D. Strintzi, *Phys. Rev. Lett.* **98**, 265003 (2007).
88. R. E. Waltz et al. , *Phys. Plasmas* **14**, 122507 (2007).
89. K.H. Burrell, *Plasma Phys. Control. Fusion* **36**, A291 (1994).
90. ASDEX Team, *Nucl. Fusion* **29**, 11 (1989).
91. P. Gohil, *C. R. Physique* **7**, 606 (2006).
92. U. Stroth, and M. Ramisch, *C. R. Physique* **7**, 686 (2006).
93. R. C. Wolf, *Plasma Phys. Control. Fusion* **45**, R1 (2003).
94. J.W. Connor, T. Fukuda, X. Garbet, et al., *Nucl. Fusion* **44**, R1 (2004).
95. T. Tala and X. Garbet, *C. R. Physique* **7**, 622 (2006).
96. K.H. Burrell, *Phys. Plasmas* **6**, 4418 (1999).
97. R.E. Waltz, G.D. Kerbel, J. Milovitch, *Phys. Plasmas* **1**, 2229 (1994).
98. H. Biglari, P.H. Diamond, and P.W. Terry, *Phys. Fluids* B **2**, 1 (1990).
99. F.L. Hinton and G.M. Staebler, *Phys. Fluids* **B5**, 1291 (1993).
100. S.-I. Itoh et al., *Phys. Rev. Lett.* **72**, 1200 (1994).
101. V. B. Lebedev and P. H. Diamond, *Phys. Plasmas* **4**, 1087 (1997); M.A. Malkov and P.H. Diamond, submitted.
102. S-I. Itoh, K. Itoh, and S. Toda, *Phys. Rev. Lett.* **89**, 215001 (2002).
103. S-I Itoh, K. Itoh, *Phys. Rev. Lett.* **60**, 2276 (1988).
104. J.F. Drake, Y.T. Lau, P.N. Guzdar, et al., *Phys. Rev. Lett.* **77**, 494 (1996).
105. M. Beer, G.W. Hammett, G. Rewoldt, et al., *Phys. Plasmas* **4**, 1792 (1997).
106. C. Bourdelle, W. Dorland, X. Garbet, et al., *Phys. Plasmas* **10**, 2881 (2003).
107. J. W. Connor, R.J. Hastie, and J.B. Taylor, *Phys. Rev. Lett.* **40**, 396 (1978).
108. J.F. Drake et al., *Phys. Rev. Lett.* **77**, 494 (1996).
109. B. Coppi, A. Ferreira, J-W-K Mark, J.J. Ramos, *Nucl. Fusion* **19**, 715 (1979).
110. Y. Baranov et al., *Plasma Physics and Control. Fusion* **46**, 1181 (2004).

Working for ITER

Sachiko Ishizaka

Secretary of the ITER Council, ITER Organization, CS 90 046, 13067 St Paul lez Durance Cedex, France

1. ABOUT THE ITER ORGANIZATION

Upon the entry into force of the ITER Agreement (of which the official title is "Agreement on the Establishment of the ITER International Fusion Energy Organization for the Joint Implementation of the ITER Project), the ITER Organization (ITER International Fusion Energy Organization) was established as an international organization on 24 October 2007. Its headquarters are located in Cadarache, France.

1.1. Mission

The purpose of the ITER Organization is to provide for, and to promote, cooperation as an international project among all the Members of the ITER Project.

The ITER Organization is responsible for the construction, operation and exploitation and de-activation of the ITER facilities in accordance with the technical objectives and the general design presented in the Final Report of the ITER Engineering Design Activities. It is also responsible for encouraging exploitation of the ITER facilities by laboratories, other institutions and personnel participating in fusion energy research and development of programs of the Members, and to promote public understanding and acceptance of fusion energy.

1.2. Members and the Governing Body

Seven parties, namely, China, EU, India, Japan, Korea, Russia and US, are currently participating in the project. This means that more than half of the world's population is involved.

The ultimate decision-making body of the ITER Project is the ITER Council, which comprises representatives of the seven Members. It meets twice a year to make important decisions regarding the management of the Project, such as the basic design, technical scope, schedule, overall costs and early budget etc.

The first meeting of the Council was held on 27 November 2007 at the Headquarters of the ITER Organization in Cadarache, Southern France; the second and most recent one, was held on 17 and 18 June in Aomori, Japan.

CP1095, 2nd *ITER International Summer School: Confinement*
edited by: S.-I. Itoh, S. Inagaki, M. Shindo, and M. Yagi
2009 American Institute of Physics 978-0-7354-0628-5/09/$25.00